Correlation effects in the quasi-one-dimensional charged Bose condensate

A. Gold
Laboratoire de Physique des Solides, Université Paul Sabatier, 118 Route de Narbonne, 31062 Toulouse, France

L. Calmels
Department of Physics and Astronomy, University of Wales, Cardiff CF2 3YB, United Kingdom
(Received 16 October 1997)

We describe correlation effects in the charged quasi-one-dimensional Bose condensate with parabolic confinement. Many-body effects are calculated with the sum-rule version of the Singwi, Tosi, Land, and Sjölander theory. We give numerical and analytical results for the local-field correction, the pair-distribution function, the correlation energy, and the compressibility of the Bose condensate. The results are given as a function of the Wigner-Seitz parameter r_s and the wire-width parameter b. The exact long-wavelength behavior of the plasmon dispersion is investigated using the compressibility sum rule. [S0163-1829(98)04719-5]

I. INTRODUCTION

The random-phase approximation (RPA) is a very useful theory to describe dielectric properties of quantum liquids in the high-density limit ($r_s \ll 1$ and r_s is the Wigner-Seitz parameter).[1] The local-field correction (LFC) describes corrections to the RPA due to many-body effects[2,3] and these corrections become important at intermediate and low particle density ($r_s \geqslant 1$). The LFC of a charged Bose condensate describes correlation contributions to the dielectric function: each condensed particle is surrounded by a correlation hole that modifies the response function.

The Singwi, Tosi, Land, and Sjölander[4] (STLS) theory for the LFC is an accurate theory that has been used to describe exchange and correlation effects in charged Fermi liquids. This theory was used to obtain the LFC for an electron gas in three,[4] two,[5] and one[6] dimensions. Ground-state energy and compressibility calculations compare favorably with Monte Carlo calculations. In the electron gas the ground-state energy is the sum of the kinetic energy (of the system without interaction), the exchange energy, and the correlation energy. In the Bose condensate the kinetic energy of the free system vanishes, because all particles have condensed into the lowest-energy state (no Pauli principle). The exchange energy vanishes for the same reason: the static structure factor (SSF) of the free-boson system is equal to unity. Using the definition of the ground-state energy of an electron gas the ground-state energy of a Bose condensate is simply given by the correlation energy.

In this paper we consider a Bose condensate with long-range Coulomb interaction, where all particles have condensed into the lowest-energy state. The STLS approach was used before to study the three-dimensional Bose condensate[7–9] and the two-dimensional Bose condensate.[8] The ground-state energy obtained by the STLS approach is in good agreement with Monte Carlo calculations[10–13] and hypernetted-chain calculations.[14] A sum-rule version of the STLS approach has been used to calculate the LFC of the Bose condensates in three and two dimensions.[8] This sum-rule approach is somewhat simpler than the STLS approach and gives analytical results for the LFC. It was used to study the electron gas in three dimensions[15] and one dimension.[16] The sum-rule approach is based on an analytical expression for the LFC depending on three coefficients that are determined self-consistently. For the one-dimensional electron gas it has been shown recently[16] that the sum-rule version is in very good agreement with the full STLS theory.[6]

In the following we use the sum-rule version of the STLS theory to describe correlation effects and collective modes in a quasi-one-dimensional Bose condensate with parabolic confinement. Our motivation to study this system was initiated from experimental progress in recent years on Bose condensation in atom vapors.[17,18] In the condensate of neutral atoms the interaction is of short-range nature. Collective modes according to the Bogoliubov theory have been observed recently.[19] The confinement potential in the experimental setup used for the Bose condensation is very anisotropic. Such a configuration can be considered as quasi-one-dimensional with a two-dimensional oscillator potential as the confinement potential. The possibility of a Bose condensation in one-dimensional systems was also studied theoretically and a macroscopic occupation of the lowest energy state was reported.[20] Therefore, we believe that the present theoretical study of a quasi-one-dimensional charged Bose condensate in an oscillator confinement matches experimental interest. In the near future it might be possible to study the Bose condensation of charged atoms. Independent of an experimental test of our predictions, we hope that our study helps to understand better the differences concerning many-body effects between electron systems and boson systems.

The paper is organized as follows: In Sec. II we describe the model and the theory. Results for the LFC are given in Sec. III. We calculate the pair-distribution function in Sec. IV and the correlation energy in Sec. V. We describe the dielectric function and collective modes in Sec. VI. The discussion of our results is in Sec. VII. We conclude in Sec. VIII.

II. MODEL AND THEORY

We describe an interacting one-dimensional Bose gas in the condensate phase by the Wigner-Seitz parameter r_s,

which is given by $r_s=1/(2Na^*)$. N is the particle density and $a^*=\varepsilon_L/m^*e^2$ is the effective Bohr radius defined with the background dielectric constant ε_L and with the boson effective mass m^* and electric charge e. For Planck's constant we use $h=2\pi$. The effective Rydberg is defined by $Ry^*=1/(2m^*a^{*2})$ and the screening wave number is given by $q_0=2/(r_s^{1/2}a^*)$.

For the confinement model, we consider a Bose condensate free to move in the z direction and confined in the (ρ,φ) directions by a parabolic confinement potential $U_c(\rho,\varphi)=\rho^2/8m^*b^4$. b is the width parameter of the wire. A positive neutralizing background ensures a global *and* a local-charge neutrality (jellium model). The wave function in the (ρ,φ) direction for the lowest-energy state is described by $\Phi(\rho,\varphi)\propto\exp[-\rho^2/4b^2]$. Accordingly, the Fourier transform of the Coulomb-interaction potential $V(q)$ is given by

$$V(q)=\frac{e^2}{2\varepsilon_L}f(qb) \tag{1a}$$

with[6]

$$f(x)=2E_1(x^2)\exp(x^2). \tag{1b}$$

$E_1(x)$ is related to the exponential-integral function.[21] The width parameter of the wire enters the theory via the interaction potential. The asymptotic behavior of the interaction potential is given by

$$f(x\ll 1)=4\ln(1/x)-2\mathbf{C}+4x^2[\ln(1/x)+(1-\mathbf{C})/2], \tag{2a}$$

where $\mathbf{C}=0.577$ is Euler's constant,[21] and by

$$f(x\gg 1)=2/x^2-2/x^4. \tag{2b}$$

In the STLS approach the LFC $G(q)$ and the SSF $S(q)$ are calculated in a self-consistent way. The self-consistency is ensured by the STLS equation that connects $G(q)$ with $S(q)$.[3] For a one-dimensional quantum liquid this equation is given by[6]

$$G(q)=\frac{1}{2\pi N}\int_{-\infty}^{\infty}dk\,\frac{q(q-k)V(q-k)}{q^2V(q)}[1-S(k)]. \tag{3}$$

For a Bose condensate the SSF is expressed in terms of the LFC as

$$S(q)=\frac{1}{\{1+4m^*NV(q)[1-G(q)]/q^2\}^{1/2}}. \tag{4}$$

With $G(q)=0$ in Eq. (4) one obtains the static structure factor $S_{\mathrm{RPA}}(q)$ within the RPA. The STLS result is given by the self-consistent numerical solution of Eqs. (3) and (4).

Within the sum-rule approach of the STLS theory the LFC is given in analytical form and is parametrized by three coefficients, which are calculated self-consistently. As for the electron gas in one dimension[16] we use for the Bose condensate the parametrization

$$G(q)=r_s\frac{a^*}{\pi bC_2}\frac{f([q^2b^2-C_3q_0|q|b^2+q_0^2b^2/C_1^2]^{1/2})}{f(qb)}. \tag{5}$$

The self-consistent calculation of $C_1=C_1(r_s,b)$, $C_2=C_2(r_s,b)$, and $C_3=C_3(r_s,b)$ is obtained from the STLS equation for $q\to 0$, $q=q_0$, and $q\to\infty$: The coefficients depend on r_s and b and are calculated using

$$\frac{f(q_0b/C_1)}{C_2}=2\int_0^{\infty}dx[f(x)+x\,df(x)/dx][1-S(x)], \tag{6}$$

$$\frac{1}{C_2}=2\int_0^{\infty}dx[1-S(x)], \tag{7}$$

and

$$f(q_0b[1-C_3+1/C_1^2]^{1/2})/C_2 = \int_0^{\infty}dx[(1-x/q_0b)f(q_0b-x) + (1+x/q_0b)f(q_0b+x)][1-S(x)], \tag{8}$$

For details we refer the reader to Ref. 16, where we discussed the equations for a one-dimensional electron gas.

III. THE LOCAL-FIELD CORRECTION

The small and large wave-number behaviors of the LFC can be expressed analytically in the large-density limit. Using Eq. (2b) and replacing the SSF $S(q)$ by $S_{\mathrm{RPA}}(q)$ in Eqs. (6) and (7), we can derive

$$C_1(r_s\to 0)=\frac{\pi^2\Gamma(\frac{1}{4})^{1/2}b^{1/2}}{\Gamma(\frac{3}{4})^{3/2}a^{*1/2}r_s^{1/4}} \tag{9}$$

and

$$C_2(r_s\to 0)=\frac{9}{32}\frac{\pi^{1/2}br_s^{1/4}}{2^{1/4}\Gamma(\frac{7}{4})^2a^*}. \tag{10}$$

Γ is Euler's gamma function.[21] We conclude that $G(q\to 0)\propto r_s^{5/4}$ and $G(q\to\infty)\propto r_s^{3/4}$ in the small-r_s limit: the LFC for the Bose condensate can be neglected in the high-density limit $r_s\ll 1$. However, the LFC becomes important at intermediate and low particle density. In Table I we give some numerical results for the coefficients C_i $(i=1,2,3)$ calculated in the sum-rule version of the STLS theory for $b=a^*$. These coefficients are useful to express the LFC and the static structure factor in an analytical form. We remember that the full STLS theory only gives numerical results. From these coefficients one can easily check that $C_1(r_s\to 0)\propto 1/r_s^{1/4}$ and $C_2(r_s\to 0)\propto r_s^{1/4}$.

The LFC is shown in Fig. 1 for a Bose condensate of width parameter $b=a^*$ and for various values of r_s: $G(q)$ is large at low-particle density $(r_s=4)$ while $G(q)$ becomes small for high density $(r_s=0.1)$. Note that the situation is different in the high-density limit of a Fermi liquid where $G(q\to\infty)=\frac{1}{2}$ due to exchange effects.[3]

The static structure factor is shown in Fig. 2 for $b=a^*$ and various values of r_s. The effects of the LFC in the static structure factor are estimated by comparing $S(q)$ to

TABLE I. Coefficients C_1, C_2, and C_3 for the LFC of a Bose condensate of width parameter $b=a^*$ for different values of the Wigner-Seitz parameter r_s.

r_s	C_1	C_2	C_3
0.01	7.080	0.1617	0.042 94
0.02	5.910	0.1945	0.058 94
0.03	5.323	0.2171	0.070 25
0.04	4.946	0.2350	0.079 09
0.06	4.465	0.2632	0.092 53
0.08	4.157	0.2857	0.102 53
0.1	3.937	0.3048	0.110 4
0.2	3.344	0.3755	0.133 8
0.3	3.058	0.4272	0.145 4
0.4	2.881	0.4701	0.151 8
0.6	2.667	0.5420	0.157 9
0.8	2.542	0.6039	0.159 6
1	2.461	0.6600	0.159 3
2	2.319	0.9064	0.149 4
3	2.346	1.140	0.138 1
4	2.446	1.382	0.128 6
6	2.767	1.910	0.115 7
8	3.181	2.495	0.108 5
10	3.637	3.118	0.104 1
20	5.856	6.387	0.087 7

$S_{\mathrm{RPA}}(q)$: these effects are negligible at large particle density ($r_s=0.1$) while they become important in diluted systems ($r_s=4$).

IV. THE PAIR-DISTRIBUTION FUNCTION

The pair-distribution function (PDF) $g(z)$ expresses the probability to find a particle at a distance z in the presence of a particle at $z=0$.[1,2] $g(z)$ is related to the static structure factor through the Fourier transform relation by

$$g(z)=1-\frac{1}{\pi N}\int_0^\infty dq\,\cos(qz)[1-S(q)]. \qquad (11)$$

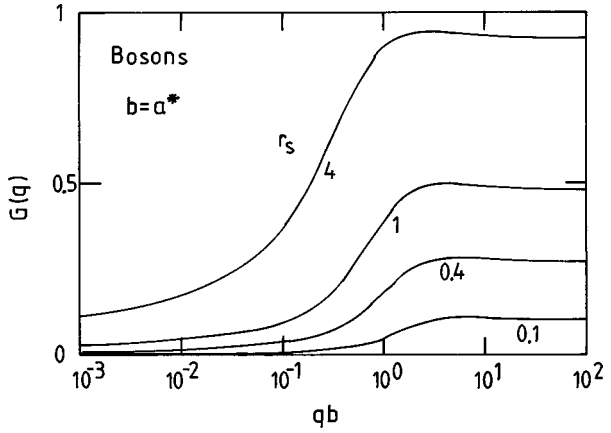

FIG. 1. Local-field correction $G(q)$ vs wave number q calculated within the sum-rule version of the STLS theory for a Bose condensate of width parameter $b=a^*$ and for $r_s=0.1$, 0.4, 1, and 4.

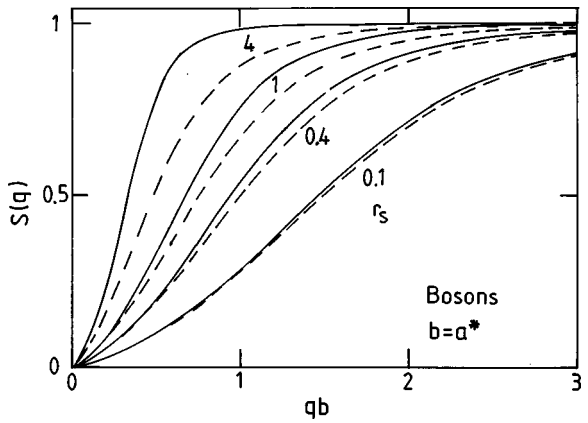

FIG. 2. Static structure factor $S(q)$ vs wave number q calculated within the sum-rule version of the STLS theory for a Bose condensate of width parameter $b=a^*$ and for $r_s=0.1$, 0.4, 1, and 4. The dashed lines represent the RPA results described by $S_{\mathrm{RPA}}(q)$.

We obtain $g_{\mathrm{RPA}}(z)$ by replacing $S(q)$ by $S_{\mathrm{RPA}}(q)$ in Eq. (11). From Eqs. (7) and (11) we can write the PDF $g(z=0)$ in terms of C_2 as[16]

$$g(z=0)=1-r_s a^*/\pi b C_2. \qquad (12)$$

The high-density behavior of $g_{\mathrm{RPA}}(z=0)$ is obtained from Eqs. (10) and (12) as

$$g_{\mathrm{RPA}}(z=0,r_s\to 0)=1-\frac{32}{9}\frac{2^{1/4}\Gamma(\frac{7}{4})^2 a^{*2}}{\pi^{3/2}b^2}\,r_s^{3/4}. \qquad (13)$$

$g(z=0)$, $g_{\mathrm{RPA}}(z=0)$, and Eq. (13) are represented in Fig. 3 for $b=a^*$. At large density, the correlation hole is small and $g(z=0)$ is correctly described by Eq. (13). The random-phase approximation becomes wrong at low density: $g_{\mathrm{RPA}}(z=0)$ is strongly negative at intermediate and large values of r_s. Some results for the PDF $g(z=0)$ are also given in Table II for various values of r_s and b. The correlation hole increases with decreasing wire width b and decreasing particle density. Note that $g(z=0)$ becomes slightly negative at very low density in the STLS approximation.

In Fig. 4 the PDF is shown versus distance z for $b=a^*$ and for $r_s=1$ and 4. The screening length $1/q_0$ is a suitable

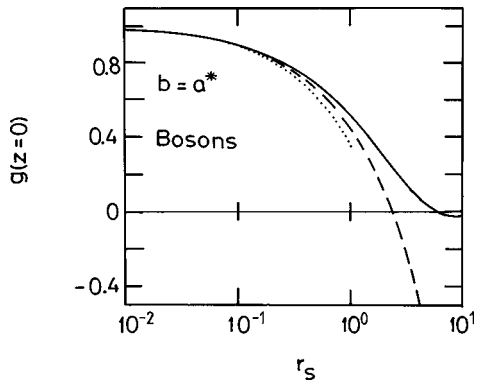

FIG. 3. Pair-distribution function $g(z=0)$ vs Wigner-Seitz parameter r_s calculated within the sum-rule version of the STLS theory (solid line) and in the random-phase approximation (dashed line) for $b=a^*$. The dotted line represents the high-density limit g_{RPA} $(z=0,\ r_s\to 0)$ as given in Eq. (13).

TABLE II. Pair-distribution function $g(z=0)$ in the sum-rule version of the STLS theory for $b=a^*/5$, $a^*/2$, a^*, $2a^*$, and for various values of r_s.

r_s	$g(z=0)$ $b=a^*/5$	$g(z=0)$ $b=a^*/2$	$g(z=0)$ $b=a^*$	$g(z=0)$ $b=2a^*$
0.1	0.800 4	0.8598	0.8956	0.9236
0.2	0.689 6	0.7760	0.8305	0.8744
0.3	0.603 6	0.7080	0.7765	0.8329
0.4	0.532 6	0.6497	0.7291	0.7960
0.6	0.419 5	0.5518	0.6477	0.7312
0.8	0.332 8	0.4714	0.5783	0.6747
1	0.264 4	0.4036	0.5177	0.6241
2	0.078 5	0.1810	0.2976	0.4277
3	0.015 1	0.0705	0.1624	0.2895
4	−0.004 5	0.0176	0.0786	0.1886
6	−0.007 4	−0.0132	0.0000	0.0614
8	−0.002 3	−0.0122	−0.0208	−0.0021
10	0.001 93	−0.0060	−0.0210	−0.0294
20	0.007 75	0.0090	0.0033	−0.0211

length scale to describe the correlation hole: $g(z)$ approaches unity for $q_0 z \approx 10$ independently of r_s. At intermediate distance ($10 < q_0 z < 30$), $g(z)$ passes through a smooth maximum and a smooth minimum before approaching unity. For a very large distance, $g(z)$ behaves approximately as

$$g(z\to\infty) = 1 - A/(q_0 z)^2 + O(1/(q_0 z)^{5/2}). \tag{14}$$

Note that this analytical expression is not an exact result. Equation (14) was obtained by fitting our numerical results for $g(z)$. Nevertheless, Eq. (14) accurately describes the PDF for $10^2 < q_0 z < 10^4$, see the inset in Fig. 4. The coefficient A in Eq. (14) is given in Table III for $b=a^*$ and various values of r_s.

V. THE GROUND-STATE ENERGY

The correlation energy per particle (which is identical to the ground-state energy per particle) of a one-dimensional

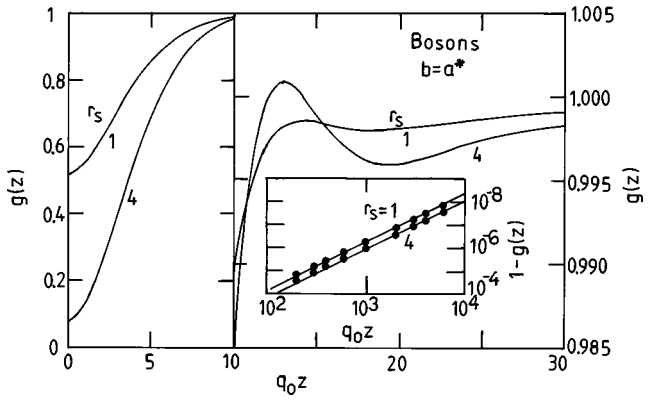

FIG. 4. Pair-distribution function $g(z)$ vs interparticle distance z in the sum-rule version of the STLS theory for $b=a^*$ and for $r_s=1$ and 4. The inset describes the large-distance behavior given by Eq. (14) (solid lines) and by the sum-rule version of the STLS theory (solid dots).

Base condensate is obtained from a wave number *and* coupling constant integral of the static structure factor[16]

$$\varepsilon_{\rm cor}(r_s)/Ry^* = -\frac{a^*}{2\pi}\int_0^1 d\lambda \int_0^\infty dq\; f(qb)[1-S(q,\lambda)]. \tag{15}$$

$S(q,\lambda)$ in Eq. (15) is the SSF for the coupling constant λ or for the interaction potential $V(q,\lambda)=\lambda V(q)$. In other words, one has to calculate the LFC for each value of the coupling constant to obtain $\varepsilon_{\rm cor}(r_s)$. The λ integration in Eq. (15) becomes trivial if the LFC is neglected. One obtains the correlation energy in the random-phase approximation as[22]

$$\varepsilon_{\rm cor,RPA}(r_s)/Ry^* = -\frac{a^*}{2\pi}\int_0^\infty dq\; f(qb)\left\{1+\frac{2r_s(qa^*)^2}{f(qb)} \times\left[1-\left(1+\frac{f(qb)}{r_s(qa^*)^2}\right)^{1/2}\right]\right\}. \tag{16}$$

From Eqs. (2b) and (16) we can derive the high-density behavior of $\varepsilon_{\rm cor,RPA}$ as

$$\varepsilon_{\rm cor,RPA}(r_s\to 0)/Ry^* = -\frac{a^*}{2\pi b}B + \frac{1}{3}\frac{\Gamma(\frac{1}{4})^2 a^{*3/2}}{2^{1/4}\pi^{3/2}b^{3/2}}\, r_s^{1/4}. \tag{17a}$$

TABLE III. Coefficient A for the pair-distribution function at large interparticle distance z as given in Eq. (14) for $b=a^*$ and for various values of r_s.

r_s	A
0.1	0.142
0.4	0.268
1	0.410
4	0.817
10	1.14

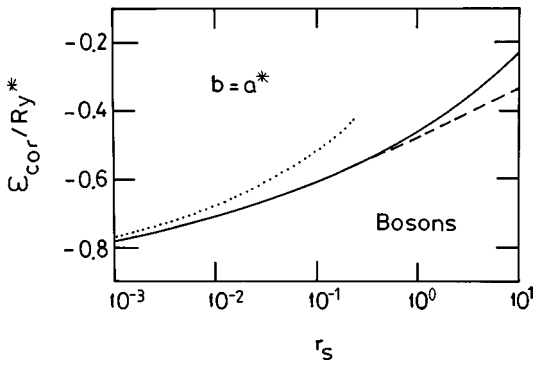

FIG. 5. Correlation energy per particle vs r_s calculated within the sum-rule version of the STLS theory (solid line) and in the random-phase approximation (dashed line) for $b=a^*$. The dotted line represents the high-density limit $\varepsilon_{\mathrm{cor,RPA}}(r_s\to 0)$ as given in Eq. (17).

B is a constant that depends on the detailed form of the interaction potential and is given by

$$B=\int_0^\infty dx\ f(x)=5.568\ 33. \tag{17b}$$

The correlation energy per particle versus r_s is shown in Fig. 5 for $b=a^*$ in the sum-rule version of the STLS theory and in the random-phase approximation. The high-density behavior within the RPA is also shown in this figure. The correlation energy is overestimated in the random-phase approximation at low carrier density: For $b=a^*$ and $r_s=10$ we obtain $\varepsilon_{\mathrm{cor}}=-0.2354Ry^*$ while the RPA gives $\varepsilon_{\mathrm{cor,RPA}}=-0.3355Ry^*$. Figure 5 indicates that the validity range of Eq. (17) is given by $r_s<0.01$.

Numerical results for the correlation energy per particle are given in Table IV for various values of r_s and b: $\varepsilon_{\mathrm{cor}}$ is less important for thick quantum wires and for dilute Bose condensates. We note that the correlation energy (the interaction energy) is negative and monotonous as a function of r_s.

The compressibility κ of a quantum liquid is an important physical quantity that contains information about many-body effects. The compressibility of an interacting one-dimensional Bose condensate is obtained from its correlation energy per particle $\varepsilon_{\mathrm{cor}}$ and given by[1,2]

$$\frac{1}{\kappa}=\frac{r_s}{2a^*}\frac{d^2\varepsilon_{\mathrm{cor}}}{dr_s^2}. \tag{18}$$

From our results for $\varepsilon_{\mathrm{cor,RPA}}(r_s\to 0)$ we derive the analytical behavior for the high-density compressibility as

$$\kappa_{\mathrm{RPA}}(r_s\to 0)=-\frac{32\ 2^{1/4}\pi^{3/2}b^{3/2}r_s^{3/4}}{\Gamma(\frac{1}{4})^2 a^{*1/2}Ry^*}. \tag{19}$$

We conclude that κ is always negative for a one-dimensional charged Bose condensate and has a larger absolute value in dilute systems and in thick wires. In Table V we give some numerical results for the compressibility for different width parameter b and Wigner-Seitz parameter r_s.

VI. DIELECTRIC FUNCTION

The plasmon dispersion $\omega_p(q)$ of a one-dimensional Bose condensate is given by the dynamical dielectric function $\varepsilon(q,\omega)$ as[1]

$$\varepsilon(q,\omega_p(q))=0. \tag{20}$$

$\varepsilon(q,\omega)$ depends on the LFC and is expressed as[2]

$$\varepsilon(q,\omega)=1+\frac{V(q)\mathbf{X}_0(q,\omega)}{1-V(q)G(q)\mathbf{X}_0(q,\omega)}, \tag{21}$$

TABLE IV. Correlation energy per particle $\varepsilon_{\mathrm{cor}}$ in units of the effective Rydberg Ry^* in the sum-rule version of the STLS theory for $b=a^*/5$, $a^*/2$, a^*, $2a^*$, and for various values of r_s.

r_s	$-\varepsilon_{\mathrm{cor}}/Ry^*$ $b=a^*/5$	$-\varepsilon_{\mathrm{cor}}/Ry^*$ $b=a^*/2$	$-\varepsilon_{\mathrm{cor}}/Ry^*$ $b=a^*$	$-\varepsilon_{\mathrm{cor}}/Ry^*$ $b=2a^*$
0.1	2.076	1.058	0.6066	0.3363
0.2	1.839	0.9701	0.5679	0.3202
0.3	1.696	0.9154	0.5434	0.3099
0.4	1.592	0.8751	0.5252	0.3021
0.6	1.443	0.8159	0.4981	0.2905
0.8	1.335	0.7720	0.4778	0.2817
1	1.250	0.7367	0.4614	0.2745
2	0.9752	0.6186	0.4055	0.2500
3	0.8121	0.5426	0.3685	0.2336
4	0.6992	0.4856	0.3398	0.2207
6	0.5510	0.4030	0.2956	0.2004
8	0.4574	0.3456	0.2620	0.1841
10	0.3928	0.3029	0.2354	0.1704
12	0.3454	0.2703	0.2139	0.1585
14	0.3089	0.2445	0.1961	0.1482
20	0.2370	0.1917	0.1578	0.1241

TABLE V. Compressibility κ (in units of a^*/Ry^*) in the sum-rule version of the STLS theory for $b = a^*/5$, $a^*/2$, a^*, $2a^*$, and for various values of r_s.

r_s	$-\kappa Ry^*/a^*$ $b=a^*/5$	$-\kappa Ry^*/a^*$ $b=a^*/2$	$-\kappa Ry^*/a^*$ $b=a^*$	$-\kappa Ry^*/a^*$ $b=2a^*$
0.25	1.50	5.86	9.60	23.40
0.5	2.92	7.79	17.64	42.31
0.75	4.29	11.28	25.22	59.80
1	5.60	14.68	32.56	76.50
1.5	8.01	21.15	46.74	108.6
2	10.16	26.99	60.17	139.4
2.5	12.07	32.25	73.11	169.6
3	13.92	36.77	84.75	198.5
3.5	15.70	40.56	95.67	227.4
4	17.53	44.00	105.0	254.3
4.5	19.45	46.99	113.0	280.3
5	21.45	49.81	119.8	304.3
5.5	23.54	52.60	125.6	326.0
6	25.76	55.51	130.5	344.6
7	30.55	61.18	138.3	377.8
8	35.80	67.54	145.6	400.3
9	41.55	74.47	152.2	416.0
10	47.75	82.06	159.8	426.7

where the density-density response function $\mathbf{X}_0(q,\omega)$ of the noninteracting Bose condensate is written, see Ref. 23, as

$$\mathbf{X}_0(q,\omega) = 4m^*Na^{*2}\,\frac{(qa^*)^2}{(qa^*)^4-(\omega/Ry^*)^2}. \tag{22}$$

The one-dimensional plasmon dispersion is obtained from Eq. (20) in the analytical form[23]

$$\omega_p(q)/Ry^* = qa^*\{f(qb)[1-G(q)]/r_s+(qa^*)^2\}^{1/2}. \tag{23}$$

In the long-wavelength limit, this equation becomes

$$\frac{\omega_p(q\to 0)}{Ry^*} = \frac{2}{r_s^{1/2}}\,qa^*[\ln(1/qb)+\beta]^{1/2} \tag{24}$$

where the constant β depends on the detailed interaction potential $V(q\to 0)$ and on the LFC $G(q\to 0)$. For a parabolic confinement model β is given by

$$\beta = -\mathbf{C}/2 - f(qb\to 0)G(q\to 0)/4. \tag{25}$$

Note that the LFC reduces the plasmon energy: $\beta < \beta_{\mathrm{RPA}} = -\mathbf{C}/2$.

One method to calculate β would be to use our results for the LFC as given in Table I. This method is not the best one because the STLS approach does not fulfill the compressibility sum rule and overestimates the short wave number LFC. For this reason it is better to calculate β with the compressibility sum rule and using the results for κ given in Table V. The compressibility sum rule expresses the long wavelength LFC in terms of the compressibility κ.[2] For the one-dimensional Bose condensate one gets

$$V(q\to 0)G(q\to 0) = -1/N^2\kappa. \tag{26}$$

Using Eqs. (25) and (26) we obtain

$$\beta = -\mathbf{C}/2 + r_s^2 a^*/Ry^*\kappa. \tag{27}$$

Our results for β calculated from Eq. (27) and using Table V are given in Table VI for various values of r_s and b.

The long-wavelength plasmon dispersion for the quasi-one-dimensional electron gas is also given by Eq. (24). The coefficient β for a charged Fermi liquid with parabolic confinement is given by[16]

$$\beta = \pi^2/16r_s - \mathbf{C}/2 - f(qb\to 0)G(q\to 0)/4. \tag{28}$$

This density behavior is different from the Bose condensate result [compare Eq. (25) with Eq. (28)]. We note that the one-dimensional plasmon dispersion for fermions has recently been measured by Raman spectroscopy in doped GaAs quantum wires.[24]

The static density-density response function $\mathbf{X}_0(q) = 4m^*N/q^2$ determines the static dielectric function $\varepsilon(q) = \varepsilon(q,\omega=0)$ by

$$1/\varepsilon(q) = 1 - \frac{4m^*NV(q)/q^2}{1+4m^*NV(q)[1-G(q)]/q^2}. \tag{29}$$

Note, that $4m^*NV(q)/q^2 = f(qb)/r_s(qa^*)^2$. For small wave numbers one finds $1/\varepsilon(q\to 0) = -G(q\to 0) < 0$. Within the RPA with $G(q)=0$ one finds $1/\varepsilon_{\mathrm{RPA}}(q\to 0) = q^2/4m^*NV(q\to 0) > 0$. Our numerical results for $1/\varepsilon(q)$ vs q are shown in Fig. 6 for different values of r_s. With increasing r_s the inverse dielectric function becomes increasingly negative for small and intermediate wave numbers and approaches $1/\varepsilon(q\to\infty) = 1$ for large wave numbers. The results shown in Fig. 6 have been obtained within the sum-rule version of the STLS approach. The negative value of $1/\varepsilon(q)$ is, for this reason, overestimated and a more accurate value

TABLE VI. Coefficient β for the long-wavelength plasmon dispersion for $b=a^*/5$, $a^*/2$, a^*, $2a^*$, and for various values of r_s.

r_s	$-\beta$ $b=a^*/5$	$-\beta$ $b=a^*/2$	$-\beta$ $b=a^*$	$-\beta$ $b=2a^*$
0.25	0.3304	0.2993	0.2951	0.2913
0.5	0.3744	0.3207	0.3028	0.2945
0.75	0.4199	0.3385	0.3109	0.2980
1	0.4673	0.3567	0.3193	0.3017
1.5	0.5696	0.3950	0.3367	0.3093
2	0.6823	0.4368	0.3551	0.3173
2.5	0.8064	0.4824	0.3741	0.3255
3	0.9350	0.5334	0.3948	0.3339
3.5	1.069	0.5906	0.4167	0.3425
4	1.201	0.6522	0.4410	0.3515
4.5	1.330	0.7196	0.4679	0.3609
5	1.454	0.7905	0.4974	0.3708
5.5	1.574	0.8637	0.5295	0.3814
6	1.686	0.937	0.5644	0.3931
7	1.892	1.090	0.6430	0.4183
8	2.076	1.236	0.7282	0.4485
9	2.238	1.376	0.8209	0.4833
10	2.383	1.507	0.9145	0.5230

of the short-range wave number behavior of $1/\varepsilon(q\to 0)$ can be obtained by using the compressibility sum rule.

VII. DISCUSSION

We have used a parabolic confinement potential to describe correlation effects in the quasi-one-dimensional Bose condensate. This choice is important: the short-distance interaction potential $V(z\to 0)$ and our quantitative results as given in our tables depend on the model. The qualitative results are, however, independent of the detailed form of the Coulomb interaction potential.

In real confined systems, the confinement potential gives rise to a ground subband and to several excited subbands. For the parabolic confinement model, the first excited subband is, for instance, described by the wave function $\Phi(\rho,\varphi)\propto\rho\,\exp[-\rho^2/4b^2]\exp[\pm i\varphi]$. The excited subbands play an important role in the quasi-one-dimensional electron gas: the one-subband model is only valid at low-particle density where the Fermi energy ε_F is lower than the intersubband energy ΔE_{12}. This is not the case for the one-dimensional Bose condensate: all particles have condensed into the lowest subband independently of the density and the one-subband model is always valid.

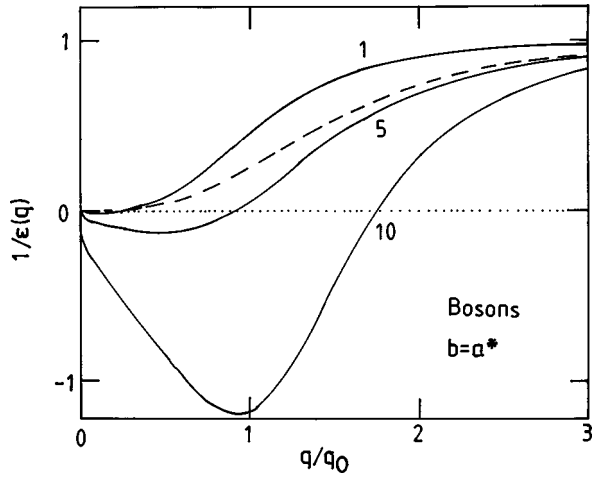

FIG. 6. Inverse dielectric function $1/\varepsilon(q)$ within the sum-rule version vs wave number q for different values of r_s. The result within the RPA is shown as the dashed line for $r_s=5$.

In this paper we presented some analytical results within the RPA, valid for high density. The results for $g_{\rm RPA}(0,r_s\to 0)$, $\varepsilon_{\rm cor,RPA}(r_s\to 0)$, $\kappa_{\rm RPA}(r_s\to 0)$, and $\beta_{\rm RPA}=-\mathbf{C}/2$ are exact and might be helpful for experimenters when Bose condensation in charged systems has been obtained. In the low-density regime the ground-state energy is modified by many-body effects described by the LFC.

In Table VII we compare for electrons and bosons the interaction energy. It is clear that with increasing Wigner-Seitz parameter the differences between bosons ($\varepsilon_{\rm int}=\varepsilon_{\rm cor}$) and electrons ($\varepsilon_{\rm int}=\varepsilon_{\rm cor}+\varepsilon_{\rm ex}$) disappear: the statistical differences between bosons and electrons become irrelevant. Similar results have been found in three and two dimensions.[10,25] From the results shown in Table VII we conclude that in the low-density limit the correlation energy

TABLE VII. Interaction energy per particle for bosons and for electrons (Ref. 16) with $b=a^*$. The interaction energy is given by $\varepsilon_{\rm int}=\varepsilon_{\rm cor}+\varepsilon_{\rm ex}$. For bosons the relation $\varepsilon_{\rm int}=\varepsilon_{\rm cor}$ holds.

r_s	boson $\varepsilon_{\rm int}/Ry^*$	electron $\varepsilon_{\rm int}/Ry^*$	electron $\varepsilon_{\rm cor}/Ry^*$
1	−0.4614	−0.5442	−0.0220
10	−0.2354	−0.2382	−0.0856
20	−0.1578	−0.1579	−0.0639

in the Bose condensate behaves as the interaction energy in Fermi systems.[16] We derive

$$\varepsilon_{\rm cor}(r_s\to\infty)/Ry^* = -0.92\,\ln\{2a^* r_s\,\exp[(3-\mathbf{C})/2]\pi b\}/r_s\,. \tag{30}$$

In the low-density limit the correlation energy is logarithmically enhanced $\varepsilon_{\rm cor}(r_s\to\infty)\propto -\ln(r_s)/r_s$ compared to three- and two-dimensional systems where $\varepsilon_{\rm cor}(r_s\to\infty)\propto -1/r_s$.

We used a jellium model where the positive neutralizing background ensures a global *and* a local-charge neutrality. In real one-dimensional confined systems, one has to take into account a local non-neutrality in directions perpendicular to the wire axis. This non-neutrality is responsible for a Hartree energy that modifies the ground-state energy.[16]

The STLS approach correctly describes the ground-state energy of charged quantum liquids. However, this theory overestimates the small wave numbers LFC and it is better to use another method to obtain $G(q\to 0)$ with accuracy. This can be done within the Vashishta and Singwi theory,[26] which has recently been used to calculate the LFC of a three-dimensional charged Bose condensate.[9]

VIII. CONCLUSION

We studied the effects of the long-range Coulomb interaction in a one-dimensional Bose condensate within the mean-field theory (RPA). Many-body effects described within the local-field correction are discussed. The LFC is given by an analytical expression depending on three coefficients, which have been calculated self-consistently. Numerical and analytical results have been given for the pair-distribution function, the correlation energy, and the compressibility. The exact long-wavelength behavior of the plasmon dispersion (collective modes) has been calculated using the compressibility sum rule. The present paper on many-body effects within the STLS approach for a Bose condensate, together with our results for electrons in Ref. 16, completes our study of many-body effects in quasi-one-dimensional systems.

ACKNOWLEDGMENTS

The ''Laboratoire de Physique des Solides'' is ''Laboratoire associé au Centre National de la Recherche Scientifique (CNRS).''

[1] D. Pines and P. Nozières, *The Theory of Quantum Liquids* (Benjamin, New York, 1966), Vol. 1.
[2] G. D. Mahan, *Many-Particles Physics* (Plenum, New York, 1991).
[3] K. S. Singwi and M. P. Tosi, Solid State Phys. **36**, 177 (1981).
[4] K. S. Singwi, M. P. Tosi, R. H. Land, and A. Sjölander, Phys. Rev. **176**, 589 (1968).
[5] M. Jonson, J. Phys. C **9**, 3055 (1976).
[6] W. I. Friesen and B. Bergersen, J. Phys. C **13**, 6627 (1980).
[7] A. A. Caparica and O. Hipolito, Phys. Rev. A **26**, 2832 (1982).
[8] A. Gold, Z. Phys. B **89**, 1 (1992).
[9] S. Conti, M. L. Chiofalo, and M. P. Tosi, J. Phys.: Condens. Matter **6**, 8795 (1994).
[10] J. P. Hansen and R. Mazighi, Phys. Rev. A **18**, 1282 (1978).
[11] D. M. Ceperly and B. J. Alder, Phys. Rev. Lett. **45**, 566 (1980).
[12] G. Sugiyama, C. Bowen, and B. J. Alder, Phys. Rev. B **46**, 13 042 (1992).
[13] S. Moroni, S. Conti, and M. P. Tosi, Phys. Rev. B **53**, 9688 (1996).
[14] V. Apaja, J. Halinen, V. Halonen, E. Krotscheck, and M. Saarela, Phys. Rev. B **55**, 12 925 (1997).
[15] A. Gold and L. Calmels, Phys. Rev. B **48**, 11 622 (1993); A. Gold, Z. Phys. B **103**, 491 (1997).
[16] L. Calmels and A. Gold, Phys. Rev. B **56**, 1762 (1997).
[17] M. H. Anderson, J. R. Ensher, M. R. Matthews, C. E. Wieman, and E. A. Cornell, Science **269**, 198 (1995).
[18] K. B. Davies, M.-O. Mewes, M. R. Andrews, N. J. van Druten, D. S. Durfee, D. M. Kurn, and W. Ketterle, Phys. Rev. Lett. **78**, 764 (1997).
[19] M. R. Andrews, D. M. Kurn, H.-J. Miesner, D. S. Durfee, C. G. Townsend, S. Inouye, and W. Ketterle, Phys. Rev. Lett. **79**, 553 (1997).
[20] W. Ketterle and N. J. van Druten, Phys. Rev. A **54**, 656 (1996).
[21] I. S. Gradshteyn and I. M. Ryzhik, *Table of Integrals, Series and Products* (Academic, New York, 1980).
[22] A. Gold and L. Calmels, Solid State Commun. **96**, 101 (1995).
[23] A. Gold, Z. Phys. B **89**, 213 (1992).
[24] A. R. Goñi, A. Pinczuk, J. S. Weiner, J. M. Calleja, B. S. Dennis, L. N. Pfeiffer, and K. W. West, Phys. Rev. Lett. **67**, 3298 (1991).
[25] A. Gold, Phys. Rev. B **50**, 4297 (1994).
[26] P. Vashishta and K. S. Singwi, Phys. Rev. B **6**, 875 (1972).